energies

MDPI

Article

Energy Efficiency Comparison of Hydraulic Accumulators and Ultracapacitors

Jorge Leon-Quiroga [1], Brittany Newell [1], Mahesh Krishnamurthy [2], Andres Gonzalez-Mancera [3] and Jose Garcia-Bravo [1,*]

[1] Purdue Polytechnic School of Engineering Technology, Purdue University, West Lafayette, IN 47907, USA; jleonqui@purdue.edu (J.L.-Q.); bnewell1@purdue.edu (B.N.)
[2] Department of Electrical and Computer Engineering, Illinois Institute of Technology, Chicago, IL 60616, USA; kmahesh@ece.iit.edu
[3] Department of Mechanical Engineering, Universidad de los Andes, Bogota 111711, Colombia; angonzal@uniandes.edu.co
* Correspondence: jmgarcia@purdue.edu

Received: 21 February 2020; Accepted: 20 March 2020; Published: 2 April 2020

Abstract: Energy regeneration systems are a key factor for improving energy efficiency in electrohydraulic machinery. This paper is focused on the study of electric energy storage systems (EESS) and hydraulic energy storage systems (HESS) for energy regeneration applications. Two test benches were designed and implemented to compare the performance of the systems under similar operating conditions. The electrical system was configured with a set of ultracapacitors, and the hydraulic system used a hydraulic accumulator. Both systems were designed to have the same energy storage capacity. Charge and discharge cycle experiments were performed for the two systems in order to compare their power density, energy density, cost, and efficiency. According to the experimentally obtained results, the power density in the hydraulic accumulator was 21.7% higher when compared with the ultracapacitors. Moreover, the cost/power ($/Watt) ratio in the hydraulic accumulator was 2.9 times smaller than a set of ultracapacitors of the same energy storage capacity. On the other hand, the energy density in the set of ultracapacitors was 9.4 times higher, and the cost/energy ($/kWh) ratio was 2.9 times smaller when compared with the hydraulic accumulator. Under the tested conditions, the estimated overall energy efficiency for the hydraulic accumulator was 87.7%, and the overall energy efficiency for the ultracapacitor was 78.7%.

Keywords: efficiency; energy storage systems; electrical power systems; hydraulic power systems; hydraulic accumulator; ultracapacitor

1. Introduction

Energy consumption in the transportation and the industrial sector represented 72% of the total energy consumption during 2018 in the United States. Most of this energy (around 87%) comes from petroleum-based sources and natural gas [1]. In the industrial sector, around 24% of the energy is spent by the agriculture, construction, and mining sectors. Many applications within these sectors use hydraulic equipment and hydraulic machinery, so improving the energy efficiency of the hydraulic systems that are already in use could have a large impact on the reduction of energy consumption and emissions. If the energy efficiency of the hydraulic machinery used in industrial applications is improved by 5%, based on the data provided by the U.S. Energy Department [1], it is possible to estimate an overall annual reduction of 1% in energy consumption in the US.

Over the last 20 years, there has been interest in developing and improving systems for energy regeneration in hydraulic machinery [2–5]. Some of the options for energy storage in energy regeneration devices include flywheels, compressed air, electrical energy storage systems (EESS), and hydraulic energy storage systems (HESS). In the electrical energy regeneration system, an electric accumulator or capacitor is used to store energy [6]. This kind of system is used in electric hybrid machinery. The return line of a boom mechanism in an excavator is connected to a hydraulic motor that is used to move an electric generator that produces electrical energy that is stored in an electric accumulator (ultracapacitor or battery) [2,3,7]. The main benefit of this system is an improvement in energy efficiency, but the complexity that is added to the baseline hydraulic system is evident. Ultracapacitors are mostly used in electric applications that require a high power density such as wind turbines in remote areas [8], energy regeneration and engine size reduction in rubber wheeled gantry cranes [9], and even biomedical applications [10].

The hydraulic energy regeneration system is similar to its electric counterpart. Instead of having an electric accumulator (ultracapacitor or battery), the hydraulic energy regeneration system uses a hydraulic accumulator that works as the energy storage device [6]. One of the main benefits when using a hydraulic regenerative system is the relative ease of installation, since the baseline application already uses a hydraulic system. Moreover, no complex power controls are needed, which is a significant advantage. On the other hand, the energy storage density in hydraulic accumulators can be a drawback when compared to a traditional electric system. Hydraulic regenerative systems have been studied for applications in relief valves [11], where the flow in the return line of the valve is used to charge a hydraulic accumulator. Alternatives like digital hydraulics have been studied to improve energy efficiency in hydraulic systems [12,13]. In these studies, a network of valves is used to change the flow rate in the actuator and to reconfigure the system in order to use the flow from assistive loads to move actuators with resistive loads.

2. Relevance of This Work

Most of the previous studies regarding EESS and HESS have focused on the characteristics of each energy storage system separately. Some studies have focused on the study of the performance of ultracapacitors [14–17] and others have focused on hydraulic accumulators. [18,19], but very little research has been done to compare the two storage systems (hydraulic accumulators and ultracapacitors) side by side. The main purpose of this study was to have a direct comparison of the performance characteristics of ultracapacitors and hydraulic accumulators when used as energy storage devices. Previous studies concerning EESS and HESS for hybrid applications have not compared the benefits and drawbacks of both systems under similar operating conditions; these studies have been focused on each system individually. For this work, an experimental procedure was developed for measuring the charging and discharging cycles of a hydraulic accumulator. Likewise, a test bench using ultracapacitors of similar energy storage capabilities was tested. The estimated energy capacity of each system was modeled with the equations shown in the following section. The experimental procedure and experimental equipment are also described in that section.

The results of this research can be used to stablish a control strategy to optimize systems that use hydraulic accumulators as energy storage systems or as a design strategy to select one over the other.

3. Test Bench Description

The main purpose of the test benches developed in this study was to compare an electrical and a hydraulic energy storage system under similar operating conditions in order to determine the efficiency, power density, energy density, and cost by energy capacity. The main characteristics of the hydraulic accumulator and the ultracapacitor used are shown below in Tables 1 and 2.

Table 1. Characteristics of the hydraulic accumulator used in this study.

Hydraulic Accumulator	
Manufacturer	**Parker Hannifin**
Reference	A2N0058D1K
Mass (kg)	4.53
Vol. Capacity (cm^3)	950
Max. Pressure (Bar)	207

Table 2. Characteristics of the ultracapacitor used in this study.

Ultracapacitor	
Manufacturer	**Maxwell Technologies**
Reference	BCAP0050 P270 S01
Mass (g)	12.2
Energy Capacity (mWh)	50.6
Max. Voltage (V)	2.7
Max. Current (A)	6.1

To compare both devices in a similar way, two test benches were designed and built. Both test benches were designed to measure charge and discharge response of the systems, which in a hydraulic system are the pressure and flow rate and in the electric system are the voltage and current.

3.1. Hydraulic Test Bench

The test bench for the hydraulic system was designed to measure the flow of energy through the accumulator while charging and discharging. The main components of the system were the battery, the electric motor, the hydraulic pump, and the hydraulic accumulator. The battery was the main source of power for the system, and it was connected to the electric motor with a DC/AC inverter. The electric motor was used to drive the hydraulic pump, which moved the fluid from the reservoir to the hydraulic accumulator. The hydraulic testbench and the DC/AC inverter are shown in Figures 1 and 2, respectively. The schematic representation of the test bench that was designed and constructed for the hydraulic accumulator is presented in Figure 3.

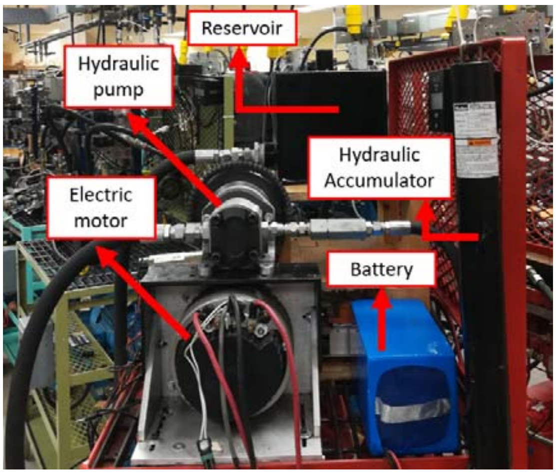

Figure 1. Hydraulic test bench.

Figure 2. DC/AC inverter used in the hydraulic test bench.

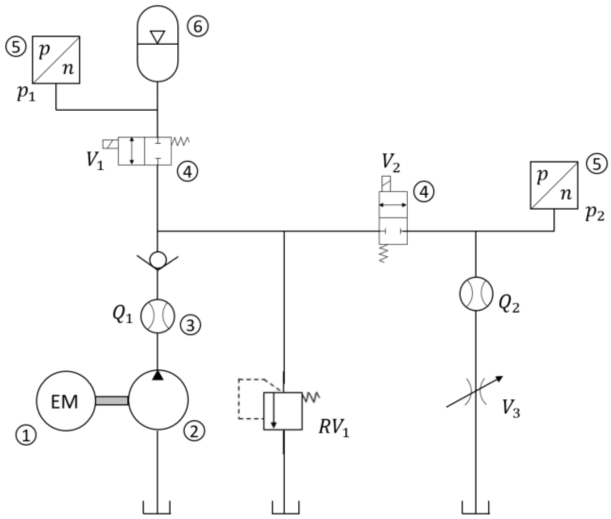

Figure 3. Schematic representation for the hydraulic accumulator test bench.

A list of the components used in the test bench is presented in Table 3.

Table 3. List of components used in the hydraulic test bench.

Index	Device	Reference	Characteristics
1	Electric motor	Motenergy 0907	Max. Speed: 5000 rpm Peak torque: 38 Nm
2	Hydraulic pump	GP-F20-12-P-A	Disp: 12 cm^3/rev Max. Flow: 40 L/min Max. Pressure: 252 Bar
3	Flow meter	FlowTech FSC 375	Max. Pressure: 6 kpsi Max. Flow: 26.45 L/min
4	V_1 and V_2	Hydraforce 12 V DC NC solenoid valve	Max. Flow: 56.7 L/min Max. Pressure: 3 kpsi
5	Pressure gage	Wika A-10	Max. Pressure: 5 kpsi Signal output: 4 to 20 mA
6	Hydraulic accumulator	Parker A2N0058D1K	Capacity: 58 in^3 Max. Pressure: 3 kpsi Precharge pressure: 1 kpsi

The test bench could be operated in either the charging or discharging modes. During charging mode, the electric AC motor was turned on and was used to move the hydraulic pump. Valve V_1 was switched on, allowing flow to go through the accumulator while valve V_2 was closed. The relief valve RV1 was closed unless a relief pressure of 3000 psi was reached. A schematic representation of the test bench during charging mode is presented in Figure 4. The red lines show the high-pressure lines.

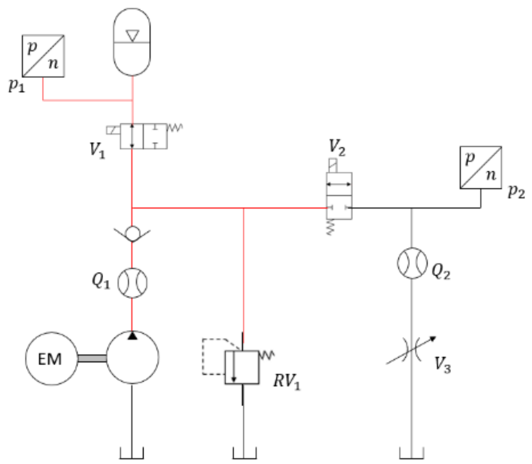

Figure 4. Hydraulic test bench during charging mode.

During charging mode, the measured variables were the current and voltage from the battery connected to the electric AC motor powering the pump and the pressure and flow rate going to the accumulator. The battery and the AC motor were connected through a DC/AC inverter. With these variables, it was possible to calculate the power input from the battery, the power going to the accumulator, the consumption of electric energy, and the energy saved in the accumulator. The speed of the electric motor was changed with a motor controller, which was connected between the battery and the electric motor. The schematic representation of the electric system used to power the pump is shown in Figure 5. The technical data of the battery, the inverter, and the electric motor are shown in Table 4.

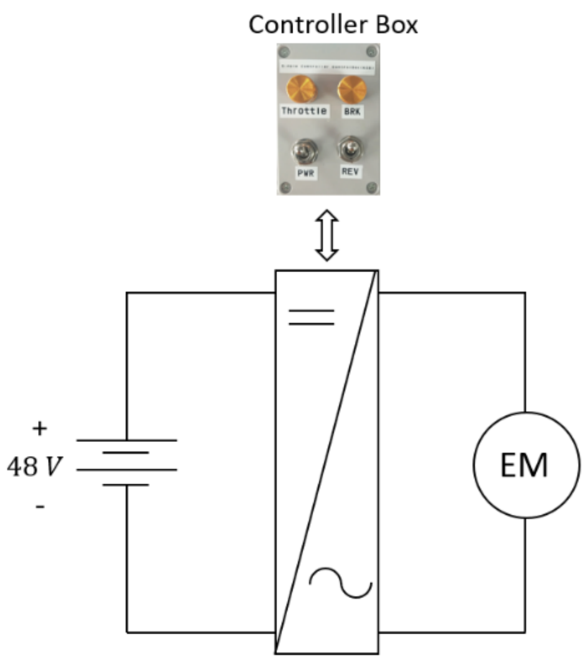

Figure 5. Schematic representation of the electric system.

Table 4. Technical data of the electric system.

Device	Reference	Characteristics
Electric motor	Motenergy 0907	Max. Speed: 5000 rpm Peak torque: 38 Nm Continuous current of 80 Amps AC Inductance phase to phase: 0.1 millihenry
Inverter	KEB48600	Max. Power: 6 kW Max. voltage: 48 V Max. Current: 125 A
Battery	SUN-CYCLE LiFePO4 48 V 24 Ah	Max. Voltage: 48 V Max. discharge current: 60 A Weight: 9.8 kg

To measure the efficiency of the hydraulic accumulator, a similar test for the discharge cycle was developed. In the discharge test, the output load was simulated with a variable orifice, V_3. The load applied to the hydraulic system increased when V_3 was progressively closed. A no-load condition was simulated when the valve was completely open. A schematic representation of the system during discharge mode is presented in Figure 6.

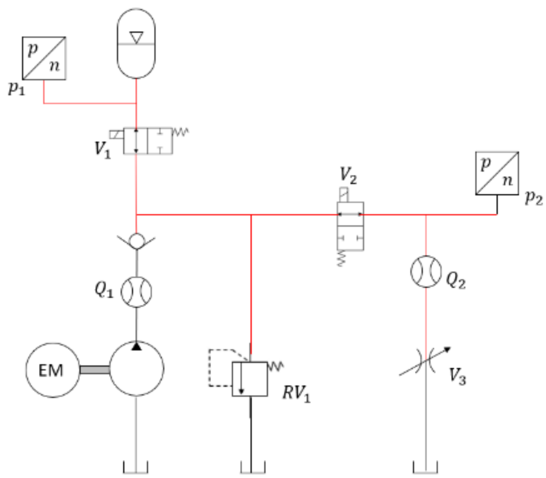

Figure 6. Hydraulic test bench during discharging mode.

To discharge the accumulator, valves V_1 and V_2 were open, while the orifice was open just between 0% and 10%. The measured variables during the discharge mode were the pressure and the flow rate just before the orifice; with these variables, it was possible to calculate the instantaneous hydraulic power used from the accumulator. The output power could be calculated by multiplying the flow rate and the pressure, and the efficiency of the hydraulic accumulator could be derived. Equations (1) and (2) were used to calculate the power input and power output in the accumulator, and Equation (3) was used to calculate the efficiency, the nomenclature shown in Table 5 describes the variables used. The results for a single test are shown in Figure 7 as a reference.

$$P_{In} = Q_{In} p_{Acc,In} \tag{1}$$

$$P_{Out} = Q_{Out} p_{Acc,Out} \tag{2}$$

$$\eta_{Acc} = \frac{\int Q_{Out} p_{Acc,Out} dt}{\int Q_{In} p_{Acc,In} dt} \tag{3}$$

Table 5. Variables used for determining the instantaneous efficiency of the accumulator.

Variable	Description
P_{In} (W)	Power charging the accumulator
P_{Out} (W)	Power discharging the accumulator
Q_{In} (gal/min)	Volumetric flow charging the accumulator
Q_{Out} (gal/min)	Volumetric flow discharging the accumulator
$p_{Acc,In}$ (psi)	Pressure charging the accumulator
$p_{Acc,Out}$ (psi)	Pressure discharging the accumulator
η_{Acc}	Efficiency of the accumulator

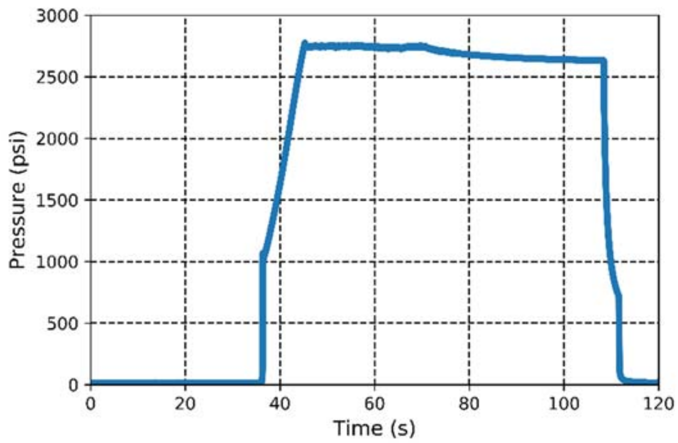

Figure 7. Pressure in the accumulator during the charging and discharging process.

The results for pressure and flow rate in the accumulator during charging are shown in Figure 8. This plot shows a sudden rise in pressure when V_1 was opened and a steady increase in pressure once the pre-charge pressure was reached. It took approximately 17 seconds to fully charge the accumulator to its maximum pressure of 2800 psi. The flow rate plot showed a sudden increase in flow rate and a decrease in flow rate once the pre-charge pressure was reached.

The results for pressure p_2 and flow rate Q_2 during discharging are shown in Figure 9. The discharge time for the accumulator was approximately 3 seconds with the valve 25% open.

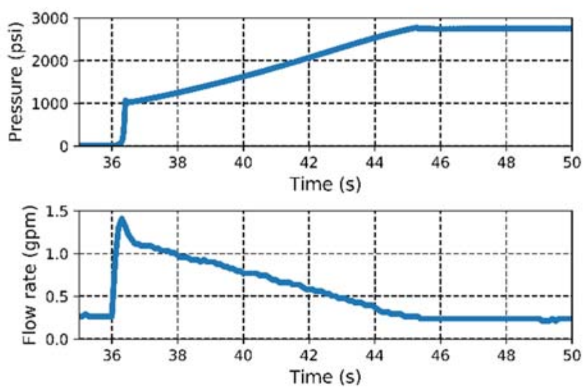

Figure 8. Pressure and flow rate while charging.

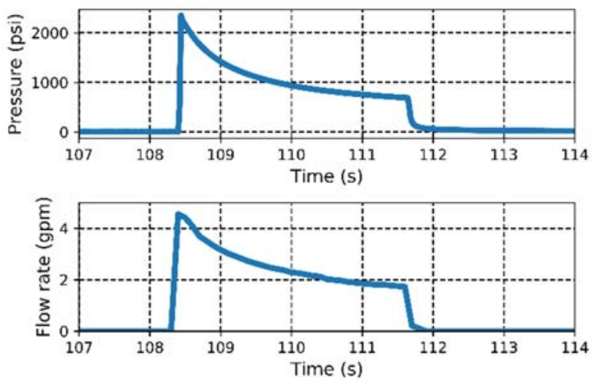

Figure 9. Pressure and flow rate while discharging.

Several experiments like the one described in this section were carried out to calculate the efficiency and performance of the hydraulic accumulator. Load conditions were changed in all the experiments by changing the orifice area. A list of the experiments is shown in Table 6. The 100% value for the orifice area was 11.7 mm^2.

Table 6. List of experiments performed in the hydraulic test bench.

Orifice Area While Charging	Orifice Area While Discharging	Orifice Area While Charging	Orifice Area While Discharging
3.1%	3.1% 6.2% 9.4% 12.5% 25.0% 100.0%	12.5%	3.1% 6.2% 9.4% 12.5% 25.0% 100.0%
6.2%	3.1% 6.2% 9.4% 12.5% 25.0% 100.0%	25.0%	3.1% 6.2% 9.4% 12.5% 25.0% 100.0%
9.4%	3.1% 6.2% 9.4% 12.5% 25.0% 100.0%	100.0%	3.1% 6.2% 9.4% 12.5% 25.0% 100.0%

3.2. Electric Test Bench

To compare the hydraulic accumulator with the ultracapacitor set, an electric test bench was designed and constructed. A schematic representation of the test bench is presented in Figure 10.

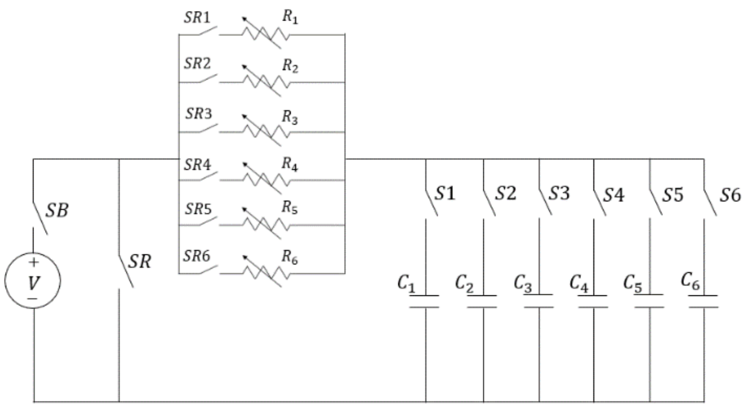

Figure 10. Schematic representation of the test bench used for ultracapacitors.

The ultracapacitors and the rheostats are shown in Figures 11 and 12, respectively.

Figure 11. Ultracapacitors used in the electric test bench.

Figure 12. Resistor bank used in the electric test bench.

This test bench was designed to measure the flow of energy through the ultracapacitors during charging and discharging. The resistance or load was made using a bank of resistors connected in parallel, which made the value of the resistance variable and easy to adjust manually. The ultracapacitor arrangement had six cells connected in series in a balancing board and six of these boards connected in parallel, so the total number of ultracapacitors used was 36. This number was selected based on calculations for the energy storage capacity for hydraulic accumulators and ultracapacitors. The selection of 36 ultracapacitors made the energy storage capacity comparable between the two systems. Switches S1 to S6 were used to activate the boards connected in parallel.

As mentioned previously, the number of ultracapacitors used in the test bench was based on the theoretical calculations for energy storage capacity in both systems. Energy stored in a hydraulic accumulator can be calculated with the following equation:

$$E_{acc} = -\int_{v_o}^{v_f} p dv \tag{4}$$

In Equation (4), E_{acc} is the total energy storage capacity of the hydraulic accumulator, p is the pressure, v_0 is the initial volume, and v_f is the final volume. The charging and discharging process of the accumulator can be assumed as adiabatic, and the polytropic index of nitrogen can be assumed as 1.4, according to Rabie [20], so the relationship between pressure and the volume in the hydraulic accumulator can be expressed as follows:

$$pv^n = p_0 v_0^n \tag{5}$$

Plugging Equation (5) into Equation (4) to obtain Equation (6):

$$E_{acc} = \int_{V_o}^{V_f} p_0 v_0^n v^{-n} dv$$

$$E_{acc} = p_0 v_0^n \left. \frac{v^{1-n}}{1-n} \right|_{v_0}^{v_f}$$

$$E_{acc} = \frac{p_0 v_0^n}{1-n}\left[v_f^{1-n} - v_0^{1-n}\right] \tag{6}$$

The final compressed volume can be expressed as a function of the maximum pressure in the accumulator.

$$p_{max} v_f^n = p_0 v_0^n$$

$$v_f = \left(\frac{p_0}{p_{max}}\right)^{1/n} v_0 \tag{7}$$

The final equation for energy in the accumulator can be obtained by plugging Equation (7) into Equation (6). Equation (8) is the expression for the energy in the hydraulic accumulator:

$$E_{acc} = \frac{p_0 v_0}{n-1}\left[\left(\frac{p_0}{p_{max}}\right)^{\frac{1-n}{n}} - 1\right] \tag{8}$$

In Equation (8), p_0 is the precharge pressure in the hydraulic accumulator, v_0 is the initial gas volume, p_{max} is the maximum pressure, and n is the ideal gas constant. The values used for the calculation of energy capacity in the hydraulic accumulator are shown in Table 7.

Table 7. Estimated energy capacity of the hydraulic accumulator.

Variable	Value
p_0 (psi)	1000
p_{max} (psi)	3000
n	1.4
v_0 (liter)	1
E_{acc} (Wh)	1.77

The energy storage capacity of the ultracapacitor arrangement needs to be approximately equal to the energy estimated from Equation (8) for the systems to be comparable. The energy in an ultracapacitor can be calculated with Equation (9):

$$E_{ult} = \frac{1}{2} C {V_{ut}}^2 \tag{9}$$

In Equation (9), C is the capacitance and V_{ut} is the voltage of the ultracapacitors. The capacitance and the voltage of the arrangement can be calculated as function of the number of cells in series (N_C) and the number of boards in parallel (N_B) with Equations (10) and (11):

$$C = \frac{N_B}{N_C} C_{cell} \tag{10}$$

$$V_{ut} = N_C V_{cell} \tag{11}$$

The total energy in the ultracapacitor arrangement can be calculated with Equation (12):

$$E_{ult} = \frac{1}{2} C_{cell} {V_{cell}}^2 (N_B N_C) \tag{12}$$

The energy capacity of the ultracapacitors is close to the energy capacity in an accumulator with six cells connected in series in a single board and six boards connected in parallel. The estimated energy storage capacity of the ultracapacitor arrangement is shown in Table 8.

Table 8. Estimated energy capacity of the ultracapacitors.

Variable	Value
C_{cell} (F)	50
V_{cell} (V)	2.7
N_B	6
N_C	6
E_{ult}(Wh)	1.82

As mentioned previously, this test bench was designed to measure the flow of energy through the ultracapacitors while charging and discharging. During charging mode, switch SB was on (see Figure 10), while switch SR was off. The current in the circuit depended on the value of the resistance. During discharge mode, switch SB was turned off and switch SR was turned on, which allowed the current to flow from the ultracapacitors to the rheostats, where the energy stored was dissipated as heat. During the experiments, the measured variables included voltage across the ultracapacitors and the current flowing through them. With these variables, the instantaneous power could be calculated, and the energy stored in the ultracapacitors could be estimated. The results for a charge and discharge experiment are shown in Figure 13 to illustrate the output.

Sixty experiments (30 for charge and 30 for discharge) like the one described in this section were made to calculate the efficiency and performance of the ultracapacitor arrangement. In the first round of experiments, just one board with six cells was connected, and five different values of resistance were tested. For the second round of experiments, two boards were connected and five different values of resistance were tested, this process was carried out until six boards were connected and tested with five different values of resistance. The same procedure was applied for discharge. The details for the tests performed in the electric testbench are summarized in Table 9; the number of boards connected, the equivalent capacitance (C), and the equivalent resistance (R) are presented in the table. A detailed explanation of the results is included in the next sections.

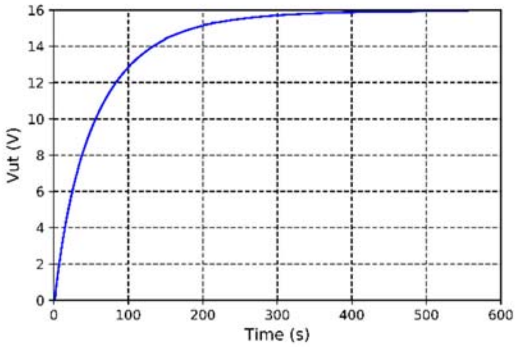

(**a**)

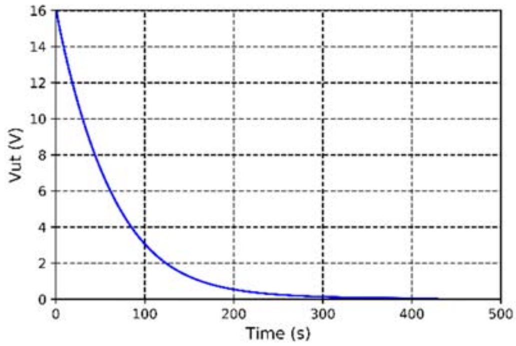

(**b**)

Figure 13. Results for charging (**a**) and discharging (**b**).

Table 9. Information of the tests performed in the ultracapacitor test bench.

Number of Boards Connected	C (F)	R (Ω)	Number of Boards Connected	C (F)	R (Ω)
		7.7			7.7
		6			6
1	8.33	4.3	4	33.32	4.3
		2.1			2.1
		1.6			1.6
		7.7			7.7
		6			6
2	16.66	4.3	5	41.65	4.3
		2.1			2.1
		1.6			1.6
		7.7			7.7
		6			6
3	24.99	4.3	6	50	4.3
		2.1			2.1
		1.6			1.6

4. Results for the Hydraulic Accumulator

Instantaneous power in the accumulator could be calculated as the product of pressure and flow rate. These variables were measured during charging and discharging. The results for energy calculation and energy efficiency for the hydraulic accumulator are shown in Table 10. The energy cycle efficiency is the ratio between the total energy released while discharging and the total energy stored while charging.

Table 10. Results for energy calculation in the hydraulic accumulator.

Variable	Value
Total Energy Stored While Charging	1.308 ± 0.003 Wh
Total energy released while discharging	1.147 ± 0.005 Wh
Energy cycle efficiency	87.7 ± 0.6%

The efficiency of the hydraulic system in transferring power from the shaft of the hydraulic pump to the hydraulic accumulator is shown in Table 10. For vehicular application, the kinetic energy of the wheels would move the shaft of a hydraulic pump, which would move the fluid to the hydraulic accumulator in order to absorb the kinetic energy of the vehicle. In the test bench, the wheel was replaced by an electric system. In previous studies, it has been demonstrated that using hydraulic accumulators in vehicle drivetrains can have a positive impact in the efficiency of a vehicle. Wang et al. [19] demonstrated the advantages of a simulated drivetrain for a light passenger vehicle, where, although the energy used for the simulated drive cycle was better using the pure electric drivetrain, the acceleration performance was better for the hydraulic drivetrain thanks to its higher power density. Moreover, Hui et al. [18] studied the effect of using a hydraulic accumulator for extending the state of charge of a battery when hybridizing an electric drivetrain with a hydraulic regeneration with positive results due to the high efficiency of hydraulic accumulators. The power in the hydraulic pump shaft was calculated as the product of the shaft torque and the rotational speed. The torque was estimated based on the pressure at outlet of the pump. The pressure and the torque were correlated according to the next expression.

$$T = \frac{D\Delta p}{\eta_m} \quad (13)$$

In Equation (13), η_m is the mechanical efficiency of the pump. The efficiency is a function of the pressure and the flow rate in the system, so the efficiency changes throughout the experiment. The pressure and the flow rate were measured, and with the datasheets provided by the manufacturer of the pump, it was possible to estimate the efficiency and the torque at any operating conditions. Thus, at any time in the experiment, the input power in the hydraulic pump could be estimated, as could the power going to the accumulator. Then, the instantaneous efficiency of the system could be obtained. At any instant of the experiment, the flow rate and the pressure could be measured. At the same instant, the power input could be measured. With this information, it was possible to create an efficiency map for the hydraulic accumulator, which is shown in Figure 14. The same map without the data points is shown in Figure 15. The map between datapoints was estimated with linear interpolation using the Matlab function griddata [21].

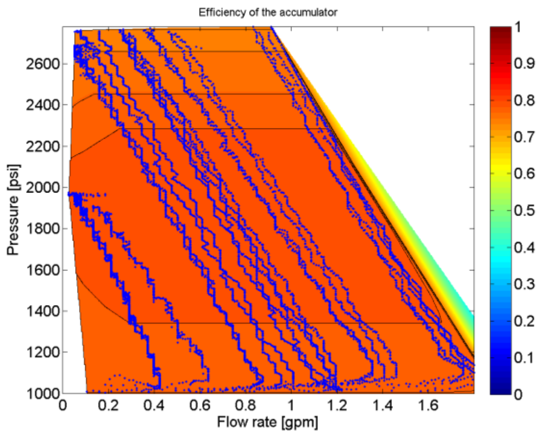

Figure 14. Instantaneous efficiency of the hydraulic accumulator with data points.

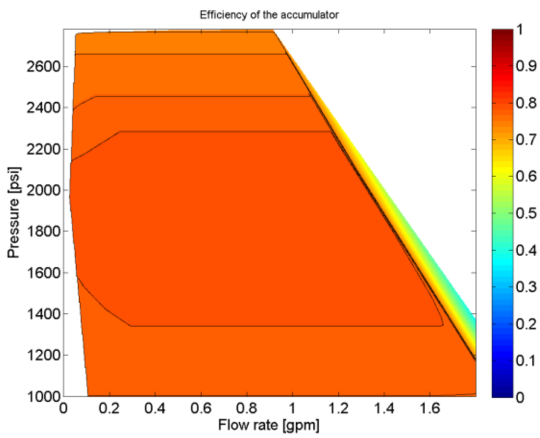

Figure 15. Instantaneous efficiency of the hydraulic accumulator using a gear pump.

The map presented in Figures 14 and 15 is important in identifying operating conditions that would be optimal for a system like the one proposed in this study. According to these plots, the highest efficiency was around 80% and was obtained for flow rates of approximately 1 gpm and pressures of approximately 1800 psi.

The current and voltage of the electric system were also measured during the experiment. A similar map of efficiency could be made for the conversion of electric power to hydraulic power. The map is shown in Figure 16.

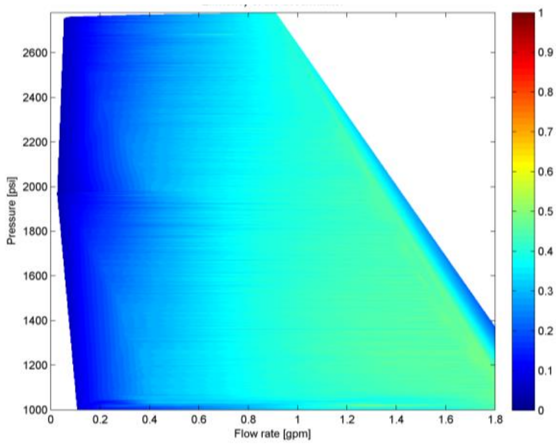

Figure 16. Instantaneous efficiency for conversion of electric power to hydraulic power.

The maximum efficiency was around 50%, relatively low because this was the efficiency of converting the electric power taken from the battery to hydraulic power in the accumulator. The electric power from the battery had to be converted into AC power in the inverter. After that, the AC power was converted into mechanical power by the electric motor. This mechanical power was used to move the shaft of the hydraulic pump, and the hydraulic pump moved the fluid from the reservoir to the accumulator through the hydraulic system, which had some power losses due to friction.

Another important aspect to consider was that the current of the battery was very high during the charging process, which was not the most efficient way to use the battery. The results for the battery for one of the charging experiments are shown in Figure 17.

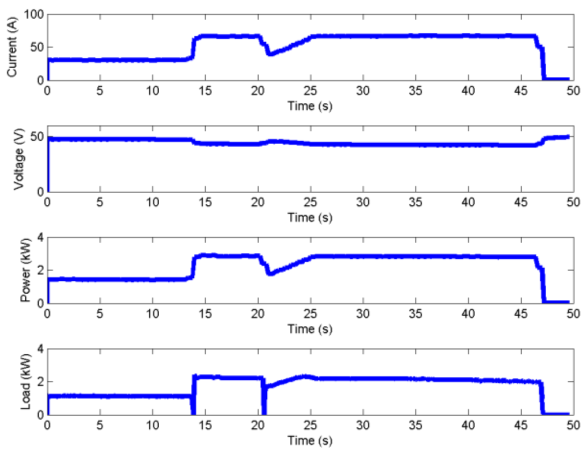

Figure 17. Experimental results for current, voltage, power, and load.

The maximum current during this experiment was 66 A, which was much higher than the continuous current recommended for the efficient operation of this battery, according to the technical data presented in Table 4. The efficiency results for a system with a model of a piston pump were estimated. The model of the piston pump was made by using commercially available datasheets of different piston pumps and then estimated with interpolation for a piston pump with a volumetric displacement of 0.73 in^3/rev, which was 11.9 cc/rev. The results of the numerical estimation are shown in Figure 18.

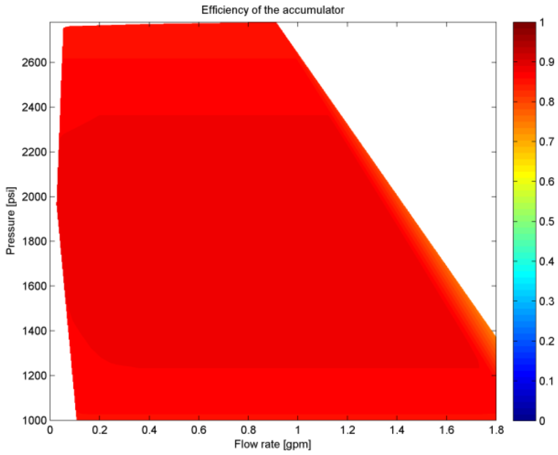

Figure 18. Instantaneous efficiency of the hydraulic accumulator using a piston pump (estimated).

The estimated results of Figure 16 show that the instantaneous efficiency of the system using a model of a piston pump could be improved, mostly because axial piston pumps had higher efficiencies. The results for the efficiency including the electric motor are shown in Figures 19 and 20. These figures show the efficiency of conversion of electric power to mechanical power in the electric system using a gear pump (experimental) and a piston pump (estimated).

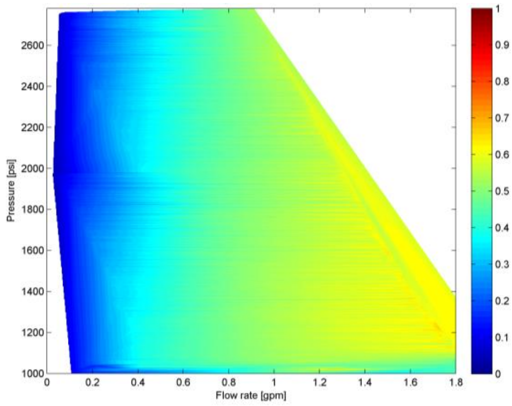

Figure 19. Efficiency of the electric system in the charging process using a gear pump.

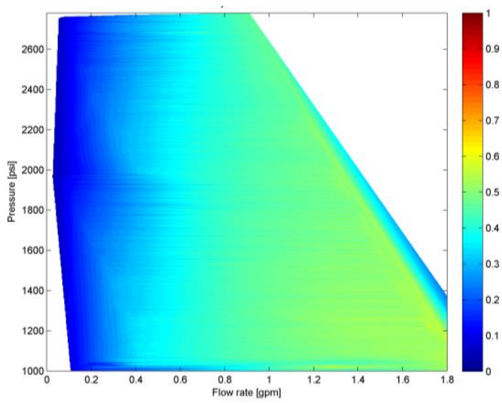

Figure 20. Efficiency of the electric system in the charging process using a piston pump (estimated).

From Figures 19 and 20, it can be observed that the electric system worked better when using a gear pump. The difference in the results was due to the input torque needed to turn the shaft of the hydraulic pump, which in this case is lower for the gear pump than for the piston pump used. The overall efficiency of the system was highly dependent on pump efficiency.

5. Results for the Ultracapacitors

The tests in the ultracapacitor test bench were made by changing the number of boards connected and the resistance used in the circuit. For each of the six possible board configurations, five different values of resistance were used. Starting with one board of six ultracapacitors, the charge and discharge tests were performed five times, and each time, the resistance selected was different. In total, thirty experiments were conducted for charging and thirty experiments for discharging. The results during charge and discharge cycles are presented below.

From Figure 21, it can be seen that the maximum voltage level of the system was reached faster when fewer boards were used—that is, when fewer ultracapacitors were energized. In Figures 21 and 22, each line represents one experiment for one value of resistance.

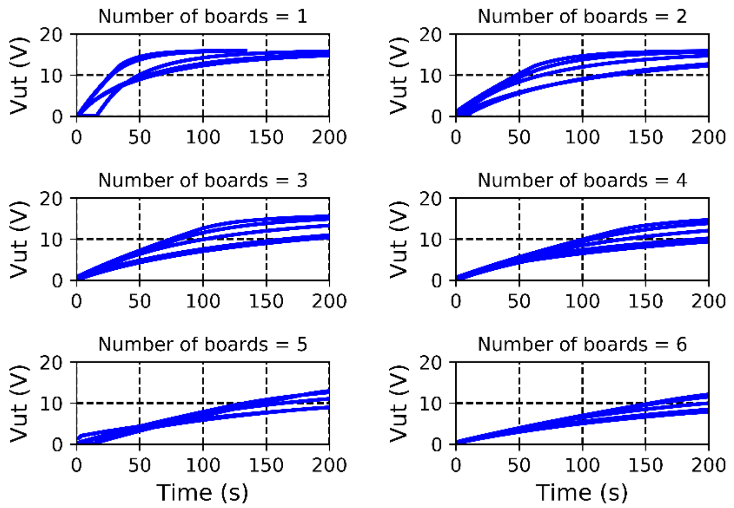

Figure 21. Voltage while charging according to the number of boards connected.

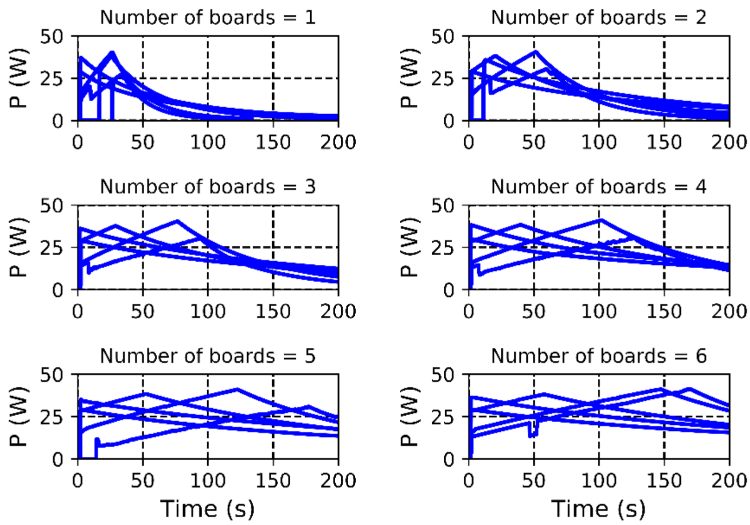

Figure 22. Power while charging according to the number of boards connected.

Now the same results are presented, but they are presented according to the number of the test (Figures 23 and 24). Test number 1 had the highest value of resistance, and test number 5 had the lowest value of resistance. The individual lines represent the number of boards connected in the electric system. The time to reach maximum voltage value was lower at a lower resistance. The value of the resistance used in each test is presented in Table 11.

Table 11. Resistance value for the tests.

Test Number	Resistance Value
Test 1	7.7 Ω
Test 2	6.0 Ω
Test 3	4.3 Ω
Test 4	2.1 Ω
Test 5	1.6 Ω

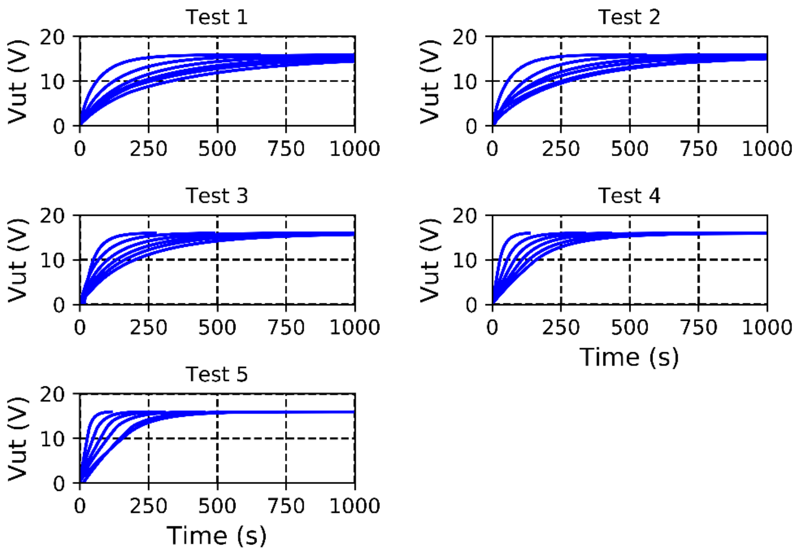

Figure 23. Voltage while charging according to the value of resistance.

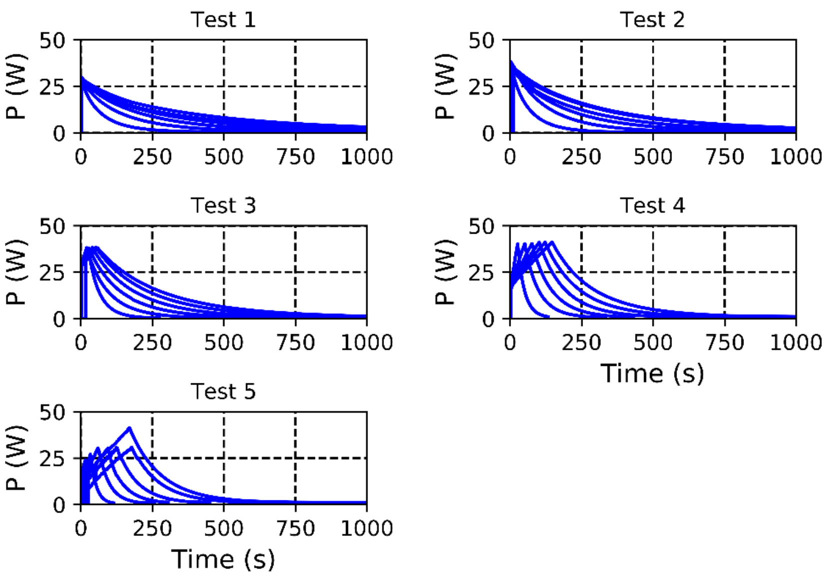

Figure 24. Power while charging according to the value of resistance.

A discharging experiment was conducted for each charging experiment. The results according to the number of boards are presented on Figures 25 and 26, and the results according the number of the test are presented in Figures 27 and 28.

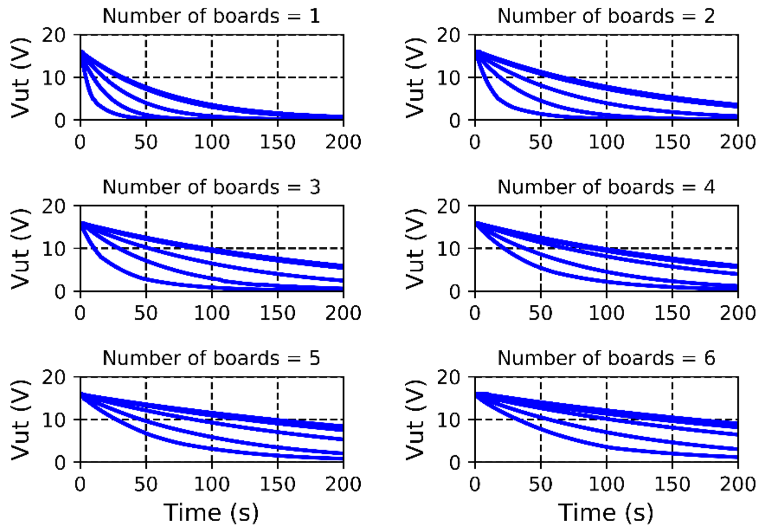

Figure 25. Voltage while discharging according to the number of boards connected.

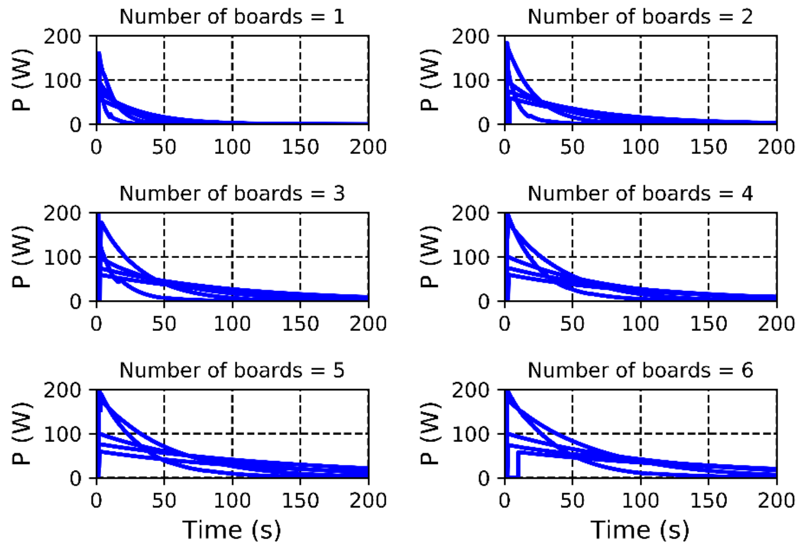

Figure 26. Power while discharging according to the number of boards connected.

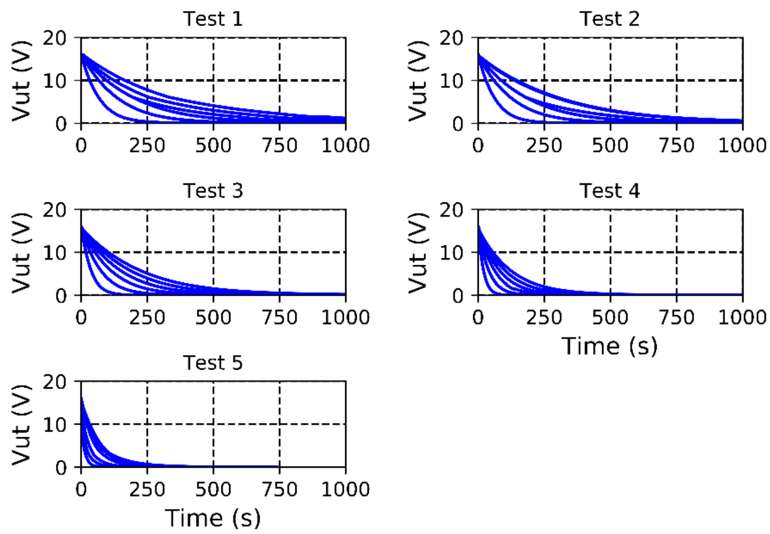

Figure 27. Voltage while discharging according to the number of the test.

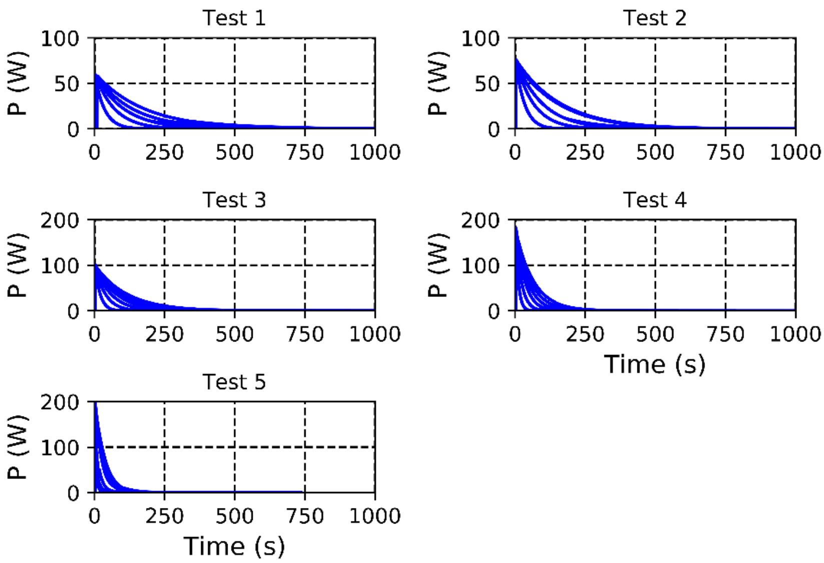

Figure 28. Power while discharging grouped according to the number of the test.

Using results presented in Figures 21–28, it was possible calculate the energy stored in the ultracapacitors and the efficiency. The results for energy calculations in the ultracapacitors are presented in Table 12.

Table 12. Results for energy calculation in the ultracapacitors.

Variable	**Number of Boards Connected in Parallel**					
	1		**2**		**3**	
	Value	**Error**	**Value**	**Error**	**Value**	**Error**
Energy stored while charging (Wh)	0.31	0.01	0.63	0.02	0.92	0.03
Energy stored while discharging (Wh)	0.25	0.01	0.50	0.01	0.76	0.02
Energy efficiency	77.46	2.33	77.2	2.7	80.75	3.3
Variable	**Number of Boards Connected in Parallel**					
	4		**5**		**6**	
	Value	**Error**	**Value**	**Error**	**Value**	**Error**
Energy saved while charging (Wh)	1.24	0.04	1.61	0.05	1.89	0.06
Energy stored while discharging (Wh)	0.97	0.03	1.29	0.04	1.47	0.05
Energy efficiency	78.99	3.91	80.4	4.73	77.74	5.42

6. Comparative Evaluation

The results for energy density and power density are presented in Table 13. Three energy systems were compared: a battery, which is the principal source of energy, the ultracapacitor, and the hydraulic accumulator.

Table 13. Energy density and power density.

Energy Storage System	Energy/Vol (Wh/m^3)	Energy/Mass (Wh/kg)	Cost/Energy (US$/Wh)
Battery	195144	115.2	0.45
Ultracapacitor	2539.7	2.72	138.67
Accumulator	1227	0.29	404.68
Energy Storage System	**Power/Vol (kW/m^3)**	**Power/Mass (kW/kg)**	**Cost/Power (US$/kW)**
Battery	325.24	0.192	270.83
Ultracapacitor	2588	2.21	217
Accumulator	7548	2.69	75

The radar plot presented in Figure 29 better illustrates these results. The radar plot shows the results in a scale from 0 to 10 for the three energy storage systems used in this study. The "*Score*" value for each component of the radar plot was determined using this equation:

$$Score = \frac{System\ Value}{Best\ Value} \cdot 10 \tag{14}$$

In Equation (14), the "*System Value*" is the value of each system: battery, ultracapacitor, or accumulator, and "*Best Value*" is the best value among the three energy storage systems. This "*Best Value*" depends on the specific characteristic to be studied. For instance, in energy/volume, the "*Best Value*" would be the highest value among the three systems, but in cost/power, the "*Best Value*" will be lowest.

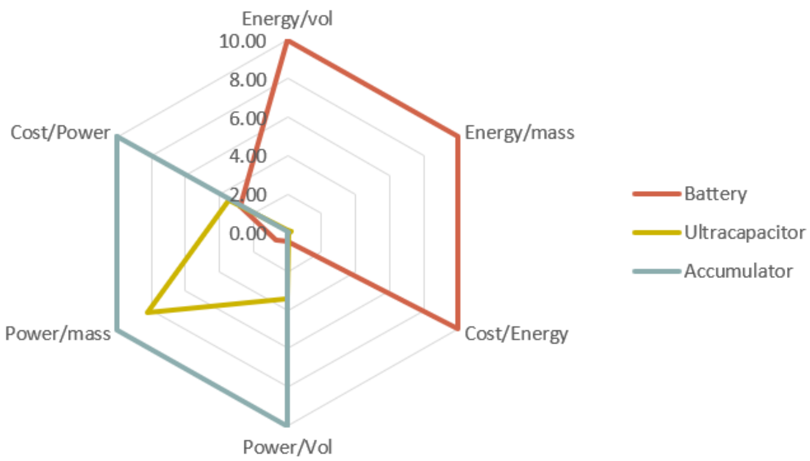

Figure 29. Radar plot comparing three energy storage systems.

From the radar plot, it is possible to see that the energy side of the plot is mostly covered by the battery. Neither of the other two systems could compete against the battery in terms of energy storage. On the other hand, the hydraulic accumulator dominates the power part of the plot. This means that the hydraulic accumulator is suited for high power applications. A comparison between the hydraulic accumulator and the ultracapacitor is shown in Figure 30.

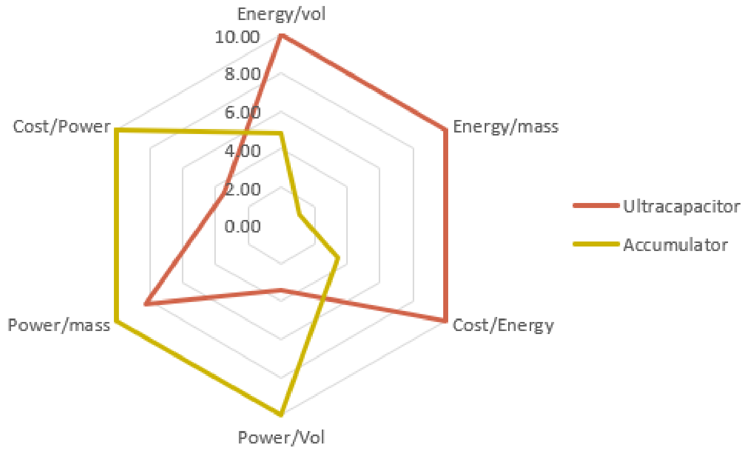

Figure 30. Radar plot comparing ultracapacitors and hydraulic accumulators.

From Figure 29, it is possible to see that the hydraulic accumulator is more suitable than the ultracapacitors in the power segment of the plot, while the ultracapacitor is better in the energy segment of the plot. However, the battery was better than these two systems for storing energy. It is important to note that the energy efficiency for the ultracapacitor was around 78.7%, and the energy efficiency of the hydraulic accumulator was 87.7%. This improvement in energy efficiency and the better power density compared with ultracapacitors could be a determining factor in choosing a hydraulic system over an electric system for a specific application when needing to rapidly charge or discharge energy storage devices, such as in the case for regenerative breaking.

The net cost of each system is presented in Table 14, but the information of this table is not enough to make an effective cost analysis of the energy storage systems considered in this study. It is necessary to consider the results presented in Table 14 and in the radar plots of Figures 29 and 30.

Table 14. Cost of each system.

Energy Storage System	Cost
Battery	390 USD
Ultracapacitors	210 USD
Hydraulic accumulator	391 USD

From the comparative results presented in the radar plots of Figures 29 and 30, it is possible to see that regarding cost/energy ratio, the battery was far better than ultracapacitors and hydraulic accumulators. The cost per unit of energy in the battery was 0.45 USD/Wh, the cost per unit of energy in the ultracapacitors was 138.7 USD/Wh, and the cost per unit of energy in the hydraulic accumulator was 404.7 USD/Wh. Regarding the cost per unit of power, the best system was the hydraulic accumulator with 75 USD/kW, the ultracapacitor had a cost/power ratio of 217 USD/kW, and the battery had a cost/power ratio of 270.8 USD. These results demonstrate the potential of hydraulic accumulators for applications that require a high power density. Nevertheless, it is necessary to consider how expensive an accumulator could be if it is required to store energy for a large period, because its cost per unit of energy is not the best.

7. Conclusions

Two test benches were designed and built to test two different energy storage systems: a hydraulic accumulator and an ultracapacitor with identical energy capacities. The energy efficiency under the test conditions for the hydraulic accumulator was 87.7%, and the energy efficiency of the ultracapacitor was 78.7%.

The efficiency map from this study can be used to determine a control strategy for a regenerative system with hydraulic accumulators. This efficiency map can be replicated for different hydraulic pumps by using numerical models for a pump. In addition, the analysis of the efficiency map for a piston pump shows that a hydraulic accumulator would be more efficient if a piston pump is used instead of a gear pump.

This study also shows that energy segments of the radar plot were dominated by the ultracapacitor, while the power segments were dominated by the hydraulic accumulator. It is interesting to note that there were segments in the radar plot that were not covered by either of the three energy storage systems. In other words, none of the systems showed a good score in cost/power and energy/volume. This means that energy storage systems with high energy density can provide high power but at a high cost. Moreover, there was no system with a high score in power/volume and cost/energy, which means that the energy storage systems with good power density can be used to store energy but at a high cost.

The higher energy efficiency in the hydraulic accumulator and the better power density compared with ultracapacitors could be determining factors in choosing a hydraulic system over an electric system for a specific application, where there is a need to rapidly charge or discharge energy storage devices, such as in the case of regenerative breaking.

Author Contributions: Conceptualization, J.L.-Q., J.G.-B. and M.K.; methodology, J.L.-Q., J.G.-B. and M.K.; software, J.L.-Q.; validation, J.L.-Q., B.N., M.K., A.G.-M., and J.G.-B.; formal analysis, J.L.-Q., and J.G.-B.; investigation, J.L.-Q., M.K., A.G.-M., and J.G.-B.; resources, B.N., and J.G.-B.; data curation, J.L.-Q.; writing—original draft preparation, J.L.-Q.; writing—review and editing, J.L.-Q., B.N., M.K., A.G.-M., and J.G.-B.; visualization, J.L.-Q., B.N., M.K., A.G.-M., and J.G.-B.; supervision, B.N., M.K., A.G.-M., and J.G.-B.; project administration, B.N., and J.G.-B.; funding acquisition, B.N., and J.G.-B. All authors have read and agreed to the published version of the manuscript.

Funding: This research was funded by the Purdue Polytechnic, office of the vice dean of research, and the school of Engineering Technology at Purdue University.

Acknowledgments: Special thanks for Sun Hydraulics for providing testing components.

Conflicts of Interest: The authors declare no conflict of interest.

References

1. U.S. Energy Information Administration. *Monthly Energy Review*; U.S. Energy Information Administration: Washington, DC, USA, 2019.
2. Lin, T.; Wang, Q.; Hu, B.; Gong, W. Development of hybrid powered hydraulic construction machinery. *Autom. Constr.* **2010**, *19*, 11–19. [CrossRef]
3. Kwon, T.S.; Lee, S.W.; Sul, S.K.; Park, C.G.; Kim, N.I.; Kang, B.I.; Hong, M.S. Power Control Algorithm for Hybrid Excavator with Supercapacitor. *IEEE Trans. Ind. Appl.* **2010**, *46*, 1447–1455. [CrossRef]
4. Xiao, Q.; Wang, Q.; Zhang, Y. Control strategies of power system in hybrid hydraulic excavator—ScienceDirect. *Autom. Constr.* **2018**, *17*, 361–367. [CrossRef]
5. Wang, T.; Wang, Q.; Lin, T. Improvement of boom control performance for hybrid hydraulic excavator with potential energy recovery—ScienceDirect. *Autom. Constr.* **2013**, *30*, 161–169. [CrossRef]
6. Lin, T.; Chen, Q.; Ren, H.; Huang, W.; Chen, Q.; Fu, S. Review of boom potential energy regeneration technology for hydraulic construction machinery. *Renew. Sustain. Energy Rev.* **2017**, *79*, 358–371. [CrossRef]
7. Lin, T.; Huang, W.; Ren, H.; Fu, S.; Liu, Q. New compound energy regeneration system and control strategy for hybrid hydraulic excavators. *Autom. Constr.* **2016**, *68*, 11–20. [CrossRef]
8. Tan, Y.; Ciufo, P.; Meegahapola, L.; Muttaqi, K.M. Enhanced Frequency Response Strategy for a PMSG-Based Wind Energy Conversion System Using Ultracapacitor in Remote Area Power Supply Systems. *IEEE Trans. Ind. Appl.* **2016**, *53*, 549–558. [CrossRef]
9. Kim, S.M.; Sul, S.K. Control of Rubber Tyred Gantry Crane with Energy Storage Based on Supercapacitor Bank. *IEEE Trans. Power Electron.* **2006**, *21*, 1420–1427. [CrossRef]
10. Pandey, A.; Allos, F.; Hu, A.P.; Budgett, D. Integration of supercapacitors into wirelessly charged biomedical sensors. In Proceedings of the 2011 6th IEEE Conference on Industrial Electronics and Applications, Beijing, China, 21–23 June 2011; pp. 56–61. [CrossRef]

11. Lin, T.; Zhou, S.; Chen, Q.; Fu, S. A Novel Control Strategy for an Energy Saving Hydraulic System With Near-Zero Overflowing Energy-Loss. *IEEE Access* **2018**, *6*, 33810–33818. [CrossRef]
12. Wang, B. High Speed On-Off Valve Self-adapting Clamping System. *J. Appl. Sci.* **2014**, *14*, 279–284. [CrossRef]
13. Andruch, J.; Lumkes, J.H. Regenerative Hydraulic Topographies using High Speed Valves. *SAE Tech. Pap. Ser.* **2009**. [CrossRef]
14. Fouda, M.; Elwakil, A.S.; Radwan, A.G.; Allagui, A. Power and energy analysis of fractional-order electrical energy storage devices. *Energy* **2016**, *111*, 785–792. [CrossRef]
15. Hartley, T.T.; Veillette, R.J.; Adams, J.L.; Lorenzo, C.F. Energy storage and loss in fractional-order circuit elements. *IET Circuits Devices Syst.* **2015**, *9*, 227–235. [CrossRef]
16. Allagui, A.; Freeborn, T.J.; Elwakil, A.S.; Maundy, B.J. Reevaluation of Performance of Electric Double-layer Capacitors from Constant-current Charge/Discharge and Cyclic Voltammetry. *Sci. Rep.* **2016**, *6*, 38568. [CrossRef] [PubMed]
17. Freeborn, T.J. Estimating supercapacitor performance for embedded applications using fractional-order models. *Electron. Lett.* **2016**, *52*, 1478–1480. [CrossRef]
18. Hui, S.; Lifu, Y.; Junqing, J.; Yanling, L. Control strategy of hydraulic/electric synergy system in heavy hybrid vehicles. *Energy Convers. Manag.* **2011**, *52*, 668–674. [CrossRef]
19. Wang, F. Comparison between Hydraulic Hybrid and Electric Hybrid Passenger Vehicles using ADVISOR 2004. In Proceedings of the 52nd National Conference on Fluid Power, Las Vegas, NV, USA, 23–25 March 2011; pp. 31–40.
20. Rabie, M.G. *Fluid Power Engineering*; McGraw-Hill: New York, NY, USA, 2009; Volume 28.
21. Interpolate 2-D or 3-D Scattered Data—MATLAB Griddata. Available online: https://www.mathworks.com/help/matlab/ref/griddata.html (accessed on 15 January 2020).